chemically (*25*) and overexpressed ADAMs lacking a catalytic domain can function as dominant negatives (*5*), it is unlikely that the $tace^{\Delta Zn}$ gene product, if expressed at the protein level (*26*), is functioning as a dominant negative with respect to other ADAM members because $tace^{\Delta Zn/+}$ mice have no phenotype, and shedding of various membrane proteins including TNF and L-selectin is normal in $tace^{\Delta Zn/+}$ cells (*12*).

These data suggest a critical role for TACE in the processing of multiple proteins. Although TACE could be an obligate component of a proteinase cascade, specific cleavage of processing-site peptides by TACE, and not by the structurally related metalloproteinase MMP-3 (*27, 28*), indicates that TACE may directly process multiple shed proteins. The strong interaction between TACE and a TNF peptide (cleavage was 9 times and 2250 times more efficient than with the TGFα and L-selectin peptides, respectively) could explain why TACE cleaves extracted TNF precursor protein whereas other apparent native substrates are not cleaved (*3, 28*). In these cases, membrane anchoring may be required to productively align the enzyme and its substrate (*22, 27, 29, 30*).

TACE may be a central component of the mechanism by which cells shed membrane proteins. Lethality in mice lacking TACE highlights the importance of TACE-directed ectodomain shedding during development. Although other metalloproteinases may also participate in the shedding of these apparent TACE substrates, therapeutic inhibitors of TNF release that target TACE may have activity against other shed proteins.

References and Notes

1. Disintegrin domains may encode integrin ligands that regulate intercellular and cell-matrix interactions.
2. C. P. Blobel *et al.*, *Nature* **356**, 248 (1992); T. G. Wolfsberg, P. Primakoff, D. G. Myles, J. M. White, *J. Cell. Biol.* **131**, 275 (1995).
3. R. A. Black *et al.*, *Nature* **385**, 729 (1997).
4. M. L. Moss *et al.*, *ibid.*, p. 733.
5. D. Pan and G. M. Rubin, *Cell* **90**, 271 (1997).
6. C. Wen, M. M. Metzstein, I. Greenwald, *Development* **124**, 4759 (1997).
7. N. M. Hooper, E. H. Karran, A. J. Turner, *Biochem. J.* **321**, 265 (1997).
8. J. Arribas *et al.*, *J. Biol. Chem.* **271**, 11376 (1996).
9. C. I. Brannan *et al.*, *Proc. Natl. Acad. Sci. U.S.A.* **88**, 4671 (1991); M. Grell *et al.*, *Cell* **83**, 793 (1995); T. Suda, H. Hashimoto, M. Tanaka, T. Ochi, S. Nagata, *J. Exp. Med.* **186**, 2045 (1997).
10. M. L. Heaney and D. W. Golde, *Blood* **87**, 847 (1996).
11. M. Pasparakis, L. Alexopoulou, V. Episkopou, G. Kollias, *J. Exp. Med.* **184**, 1397 (1996); M. W. Marino *et al.*, *Proc. Natl. Acad. Sci. U.S.A.* **94**, 8093 (1997); J. J. Peschon *et al.*, *J. Immunol.* **160**, 943 (1998).
12. J. J. Peschon and K. L. Stocking, data not shown.
13. M. J. Harris and M. J. McLeod, *Anat. Embryol.* **164**, 207 (1982).
14. J. J. Peschon and R. W. Boyce, data not shown.
15. N. C. Luetteke *et al.*, *Cell* **73**, 263 (1993).
16. G. B. Mann *et al.*, *ibid.*, p. 249; E. A. Berkowitz *et al.*, *Cell Growth Differ.* **7**, 1271 (1996).
17. J. Massagué, *J. Biol. Chem.* **265**, 21393 (1990).
18. S. T. Wong *et al.*, *Cell* **56**, 495 (1989); R. Brachmann *et al.*, *ibid.*, p. 691.
19. P. J. Miettinen *et al.*, *Nature* **376**, 337 (1995); M. Sibilia and E. F. Wagner, *Science* **269**, 234 (1995); D. W. Threadgill *et al.*, *ibid.*, p. 230.
20. D. C. Lee and K. M. Han, in *Peptide Growth Factors and Their Receptors*, vol. 95/II of *Handbook of Experimental Pharmacology*, M. B. Sporn and A. B. Roberts, Eds. (Springer-Verlag, Berlin, 1990), pp. 611–654; G. Raab *et al.*, *Biochem. Biophys. Res. Commun.* **204**, 592 (1994); M. Suzuki, G. Raab, M. A. Moses, C. A. Fernandez, M. Klagsbrun, *J. Biol. Chem.* **272**, 31730 (1997).
21. P. D. Crowe *et al.*, *J. Exp. Med.* **181**, 1205 (1995); T. A. Bennett, E. B. Lynam, L. A. Sklar, S. Rogelj, *J. Immunol.* **156**, 3093 (1996); C. Feehan *et al.*, *J. Biol. Chem.* **271**, 7019 (1996).
22. G. Preece, G. Murphy, A. Ager, *J. Biol. Chem.* **271**, 11634 (1996).
23. G. I. Migaki, J. Kahn, T. K. Kishimoto, *J. Exp. Med.* **182**, 549 (1995).
24. J. L. Slack, P. Reddy, R. A. Black, data not shown.
25. T. G. Wolfsberg *et al.*, *Proc. Natl. Acad. Sci. U.S.A.* **90**, 10783 (1993); C. P. Blobel, *Cell* **90**, 589 (1997).
26. Antibodies for reliably detecting endogenous murine TACE are unavailable.
27. K. Maskos *et al.*, *Proc. Natl. Acad. Sci. U.S.A.* **95**, 3408 (1998).
28. J. L. Slack and R. A. Black, data not shown.
29. S. S. Sisodia, *Proc. Natl. Acad. Sci. U.S.A.* **89**, 6075 (1992); H. J. Cheng and J. G. Flanagan, *Mol. Biol. Cell.* **5**, 943 (1994); S. B. Roberts, J. A. Ripellino, K. M. Ingalls, N. K. Robakis, K. M. Felsenstein, *J. Biol. Chem.* **269**, 3111 (1994); M. R. W. Ehlers *et al.*, *Biochemistry* **35**, 9549 (1996).
30. R. Sadhukhan, G. C. Sen, R. Ramchandran, I. Sen, *Proc. Natl. Acad. Sci. U.S.A.* **95**, 138 (1998).
31. Tissues were fixed in 10% neutral-buffered formalin, embedded in paraffin, sectioned, and stained with hematoxylin and eosin. Hair specimens were prepared as described, except that bovine serum was substituted for egg white (*15*).
32. E. P. Sandgren, N. C. Luetteke, R. D. Palmiter, R. L. Brinster, D. C. Lee, *Cell* **61**, 1121 (1990); W. E. Russell, P. J. Dempsey, S. Sitaric, A. J. Peck, R. J. Coffey Jr., *Endocrinology* **133**, 1731 (1993).
33. Single-letter abbreviations for the amino acid residues are as follows: A, Ala; C, Cys; D, Asp; E, Glu; F, Phe; G, Gly; H, His; I, Ile; K, Lys; L, Leu; M, Met; N, Asn; P, Pro; Q, Gln; R, Arg; S, Ser; T, Thr; V, Val; W, Trp; and Y, Tyr.
34. Peptides were either synthesized at Immunex (TNF, L-selectin) or obtained commercially (TGFα; SynPep). The enzyme used for the digests was a catalytic domain–polyHis construct expressed in Chinese hamster ovary cells and purified with Ni-nitrilotriacetic acid (Qiagen) and gel filtration columns (*27*). About 7 μM and 1.4 μM TACE was used for the L-selectin and TGFα peptides, respectively. All the incubations were with 0.5 mM peptide in 20 μl and were done for 0.5, 1, 2, and 4 hours at 37°C in 10 mM tris (pH 7.5). Digestion was a linear function of time in all cases, and the comparative data are based on the rates of the reactions. High-performance liquid chromatography (HPLC) analysis of products was done as described [R. A. Black *et al.*, *Biochem. Biophys. Res. Commun.* **225**, 400 (1996)]. The composition of the digests was determined by liquid chromatography/mass spectrometry (LC/MS), on a 1-mm ID Vydac C18 column with a flow rate of 50 μl/min and a linear gradient of 2% acetonitrile/min in 0.1% trifluoroacetate. LC/MS data were obtained by directing 10% of the HPLC effluent to the electrospray source of a Finnigan TSQ700 triple quadrupole mass spectrometer (San Jose, CA).
35. We thank the Immunex Animal Facility, the Flow Cytometry and Histology groups, K. Brasel, C. Willis, M. Glaccum, D. Barone, R. Blanton, K. Mohler, J. Schuh, and J. Doedens for their contributions to this work; H. Nagase of the University of Kansas Medical Center for providing MMP-3; M. Hall and G. Carlton for graphic assistance; and A. Aumell for help with manuscript preparation. Supported in part by NIH grants CA43793 (D.C.L.) and DK53804 (W.E.R.), and NSF grant MCB9729645 (W.E.R.).

25 June 1998; accepted 23 September 1998

Presolar Corundum and Spinel in Ordinary Chondrites: Origins from AGB Stars and a Supernova

Byeon-Gak Choi,* Gary R. Huss, G. J. Wasserburg, Roberto Gallino

On the basis of anomalous isotopic compositions of oxygen and magnesium, 14 oxide grains from two primitive meteorites (Bishunpur and Semarkona) have been identified as circumstellar condensates. One corundum grain has a high $^{18}O/^{16}O$ ratio and isotopic compositions of magnesium, calcium, and titanium that are compatible with a formation in ejecta of a type II supernova that was about 15 times the mass of the sun. The other grains have oxygen, magnesium, and titanium compositions that are consistent with a formation around asymptotic giant branch (AGB) stars with a range of mass and initial composition. The large range of aluminum/magnesium in circumstellar corundum and spinel is considered to reflect various stages of back-reaction between condensed corundum and gaseous magnesium in cooling stellar ejecta.

Presolar grains that were extracted from primitive meteorites existed before the formation of the solar system. Most grains are circumstellar condensates that formed in stellar ejecta. They provide a unique opportunity to study nucleosynthesis in stars and to study condensation processes in the wind of mass-losing AGB stars and in supernova ejecta. The most abundant circumstellar condensates recovered are carbon-rich phases [diamond, graphite, silicon carbide, and titanium carbide (*1, 2*)]. Presolar oxides, which should have been abundant in the solar nebula, have been difficult to identify because of the overwhelming abundance of solar-system oxides in meteorites. However, more than 100 presolar corundum (Al_2O_3) and spinel ($MgAl_2O_4$) grains have been identified on the basis of their anomalous O and Mg isotopic compositions (*3–8*). Most of these grains were interpreted to have originated from AGB stars because of their large enrichments in ^{17}O in relation to solar O (*9*) and high inferred $(^{26}Al/^{27}Al)_o$ values (subscript o denotes initial values).

Most presolar oxide grains have been identified with an ion microprobe and an automatic ion-imaging technique; these grains were recognized by substantial shifts in the $^{18}O/^{16}O$ ratio (*5–8*). However, this imaging consumes large portions of smaller grains, reducing the amount of material available for isotopic study, and would not detect grains with a near-normal $^{18}O/^{16}O$ ratio (*9*). We have developed an automated search procedure using a scanning electron microscope (SEM) and an energy dispersive x-ray detector to identify and locate grains that were dispersed on a substrate and to determine the major element abundances for each grain (*10*). The location, approximate size, and chemical composition of each grain were automatically determined, and the coordinates were easily transferred to the ion probe for isotopic analysis.

About 1.4×10^4 refractory oxide and SiC grains in acid residues from the Bishunpur and Semarkona meteorites (*11*) were identified by our automated procedure. The relative abundances of grains from this population in volume percent determined from the pixel sizes are as follows: spinel, ~76%; SiC, ~15%; hibonite, ~3%; TiO_2, ~3%; corundum, ~3% (Bishunpur and Semarkona had similar proportions). From these grains, 185 corundum, 49 spinel, 25 hibonite, and 11 TiO_2 grains were chosen for isotopic measurements by an ion microprobe. Isotopic compositions of O and Mg were used to identify presolar grains. Before isotopic measurements, the morphologies of grains were examined with an SEM. Presolar oxide grains have distinctive irregular surfaces and appear as structures that are more open or as assemblages of smaller grains (Fig. 1, A, B, and possibly C). These morphologies are similar to those of presolar SiC (*12, 13*). Some grains with normal O isotopic compositions and with no large excesses of ^{26}Mg have similar irregular surface features. These morphologies may reflect the grain growth from a vapor, which can occur in stellar outflows or in hot gaseous regimes in the solar nebula. In contrast, most isotopically normal oxide grains typically have smooth surfaces, and a few have crystal faces (Fig. 1D). These grains probably crystallized from a melt. The ability to distinguish grains that were formed by condensation from a gas from those that were formed by crystallization of a melt can help identify presolar oxides before destructive analysis.

Isotopic measurements identified 14 new presolar oxide grains (*14*). We report O and Mg compositions for these grains (Table 1), compositions of Ti for five of these grains and two previously identified grains (*3, 4*), and compositions of Ca for one grain (Table 2). These data provide insight on the source stars of oxide grains.

A corundum grain from a type II supernova (SNII). Corundum grain S-C122 is enriched in ^{18}O by a factor of 3 in relation to solar O but has only a small enrichment in ^{17}O (Figs. 2 and 3). Two stellar sources could possibly produce and preserve substantial amounts of ^{18}O: a Wolf-Rayet (WR) star and a SNII. WR stars are high-mass stars that have lost their H envelope through massive stellar winds, exposing the products of stellar nucleosynthesis at their surfaces. Oxygen-18 is produced during partial He burning, and an ^{18}O-rich stellar wind can result when the products of He burning are exposed at the surface. However, He burning also produces a large amount of ^{12}C, and the ^{18}O-rich wind would have a high C/O ratio (*15*). The formation of oxide grains is not favored under

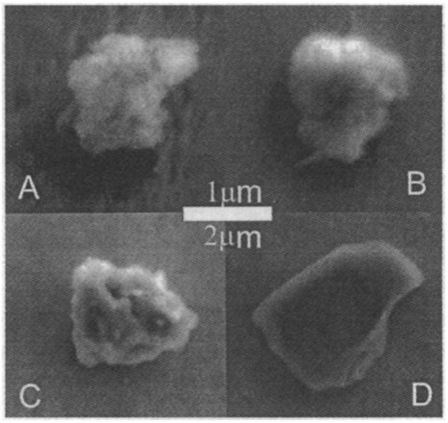

Fig. 1. SEM images of corundum grains (**A** and **B**) with anomalous O isotopic compositions and (**C** and **D**) with normal O. (A) An AGB corundum, S-C201. (B) A corundum, S-C122, inferred to be from a SN source. (C) S-C245 has normal O isotopic composition but gives a high $(^{26}Al/^{27}Al)_o$ ratio of $(3.0 \pm 2.3) \times 10^{-4}$. (D) Corundum, which was probably crystallized from a melt, with normal O and Mg isotopes. Scale bar, 1 μm for (A) and (B) and 2 μm for (C) and (D).

Table 1. O and Mg isotopic ratios and Al-Mg systematics in presolar oxide grains. In grain samples, the first and second letters represent the source meteorite (B, Bishunpur; S, Semarkona) and the mineral (C, corundum; S, spinel), respectively. The values of the terrestrial samples are from (*36*) for O and from (*37*) for Mg; measurements of the sun (solar wind or photosphere) are from (*38*). B39 and Org B data are from (*4*). Dashes indicate not applicable.

Sample	$^{17}O/^{16}O \pm 2\sigma$	$^{18}O/^{16}O \pm 2\sigma$	$^{25}Mg/^{24}Mg \pm 2\sigma$	$^{26}Mg/^{24}Mg \pm 2\sigma$	$^{27}Al/^{24}Mg \pm 2\sigma$	$(^{26}Al/^{27}Al)_o$
Terrestrial	0.0003820	0.0020052	0.12663	0.13932	—	—
Sun	<0.0021	0.0014 to 0.0031	0.122 to 0.206	0.123 to 0.215	—	—
B-C8	0.00041 ± 0.00002	0.00247 ± 0.00010	0.1281 ± 0.0032	0.1371 ± 0.0033	65 ± 7	$<1.8 \times 10^{-5}$
B-C68	0.00280 ± 0.00008	0.00205 ± 0.00013	0.1299 ± 0.0017	0.1429 ± 0.0018	59 ± 6	$6.1(\pm3.2) \times 10^{-5}$
B-C72	0.00037 ± 0.00002	0.00196 ± 0.00010	0.1275 ± 0.0024	0.1456 ± 0.0026	39 ± 4	$1.6(\pm0.7) \times 10^{-4}$
B-C129	0.00232 ± 0.00010	0.00215 ± 0.00015	0.1243 ± 0.0072	0.1943 ± 0.0096	979 ± 30	$6.1(\pm1.3) \times 10^{-5}$
B-C145	0.00037 ± 0.00003	0.00210 ± 0.00020	0.1252 ± 0.0232	0.3175 ± 0.0441	1157 ± 163	$1.5(\pm0.4) \times 10^{-4}$
B-C155	0.00110 ± 0.00002	0.00186 ± 0.00005	0.1405 ± 0.0146	0.1465 ± 0.0147	4566 ± 522	$<4.8 \times 10^{-6}$
S-C13	0.00049 ± 0.00009	0.00199 ± 0.00031	0.1269 ± 0.0082	0.1381 ± 0.0086	291 ± 31	$<2.5 \times 10^{-5}$
S-C122	0.00044 ± 0.00006	0.00634 ± 0.00039	0.1271 ± 0.0056	0.1515 ± 0.0063	20 ± 2	$6.3(\pm3.3) \times 10^{-4}$
S-C201	0.00096 ± 0.00009	0.00057 ± 0.00013	0.1238 ± 0.0103	0.1844 ± 0.0134	27 ± 3	$1.7(\pm0.5) \times 10^{-3}$
S-C203	0.00283 ± 0.00019	0.00212 ± 0.00030	0.1182 ± 0.0095	0.1613 ± 0.0116	24 ± 3	$9.3(\pm5.0) \times 10^{-4}$
S-C235	0.00177 ± 0.00006	0.00144 ± 0.00010	0.1205 ± 0.0051	0.1423 ± 0.0056	95 ± 10	$<9.1 \times 10^{-5}$
S-C245	0.00036 ± 0.00002	0.00196 ± 0.00009	0.1219 ± 0.0085	0.1524 ± 0.0098	43 ± 5	$3.0(\pm2.3) \times 10^{-4}$
S-C261	0.00299 ± 0.00010	0.00084 ± 0.00010	0.1277 ± 0.0045	0.1521 ± 0.0050	21 ± 2	$6.2(\pm2.5) \times 10^{-4}$
S-S21	0.00115 ± 0.00012	0.00171 ± 0.00026	0.1316 ± 0.0026	0.1422 ± 0.0017	4.1 ± 0.3	$7.1(\pm4.3) \times 10^{-4}$
B39	0.00260 ± 0.00006	0.00117 ± 0.00004	0.1267 ± 0.0023	0.3728 ± 0.0104	136 ± 14	$1.7(\pm0.2) \times 10^{-3}$
Org B	0.00097 ± 0.00001	0.00199 ± 0.00004	0.1573 ± 0.0160	1.8333 ± 0.0226	2027 ± 72	$8.9(\pm0.1) \times 10^{-4}$

B.-G. Choi, G. R. Huss, and G. J. Wasserburg are at the Lunatic Asylum, Division of Geological and Planetary Sciences, California Institute of Technology, Pasadena, CA 91125, USA. R. Gallino is in the Dipartimento di Fisica Generale, Università di Torino, Via P. Giuria 1, 10125 Torino, Italy.

*To whom correspondence should be addressed: E-mail: bchoi@gps.caltech.edu

such conditions (*16*). In contrast, SNII ejecta are oxygen-rich (*17*) and thus are a more likely source of S-C122.

A SNII occurs when a massive star undergoes a core collapse and explodes. During the SNII explosion, zones of different compositions from the pre-SN star are ejected, and explosive nucleosynthesis takes place in the inner zones (*17*). The bulk ejecta of a low-mass [<22 times the mass of the sun ($M_\odot$)] SNII have relatively ^{18}O-rich compositions, whereas the ejecta of a higher mass SNII produce more ^{16}O and have $^{18}O/^{16}O < (^{18}O/^{16}O)_{solar}$ (*9, 18*). However, condensation of S-C122 from bulk SNII ejecta is not plausible because the bulk ejecta would contain large anomalies in other isotopes, which were not observed. Therefore, we considered the partial mixing of various SNII zones to explain the observed isotopic compositions. This mixing approach has also been used for graphite grains (*19*).

A SNII consists of several zones, which are named for the elements that are predominantly found in these areas (*20*). The outermost zone is the H envelope of the pre-SN star, which underwent partial H burning at its base during the main sequence stage of stellar evolution. Inside the H envelope is the He/N zone, in which H burning went to completion and most CNO isotopes have been converted to ^{14}N. Aluminum-26 is very abundant in this zone. The H envelope and the He/N zone have $^{18}O/^{16}O < (^{18}O/^{16}O)_{solar}$. The H envelope has C/O < 1, but the He/N zone has C/O ≈ 1. Inside the He/N zone is the He/C zone, which is highly enriched in ^{18}O and has C/O > 1. The He/C zone also contains products of slow process (s-process) nucleosynthesis. Inside the He/C zone are the O/C and O/Ne zones, which are ^{16}O-rich. These zones also contain a mixture of the products of s-process and explosive nucleosynthesis. Zones interior to the O/C and O/Ne zones are characterized by highly anomalous isotopic compositions of many elements that are produced by explosive nucleosynthesis.

To test what mixtures can produce the characteristics of S-C122, we carried out calculations to reproduce the $^{18}O/^{16}O$ ratio in S-C122 by mixing various proportions of different SNII zones. The calculated compositions were then compared with other isotopic compositions in S-C122. We assumed that any given mixture should have C/O < 1 to condense oxides (*16*). We used yields for 15 and 25 $M_\odot$ SNII of solar metallicity ($Z_\odot = 0.02$) from (*17*), but we did not use the ^{17}O abundance in this calculation because the ^{17}O yields are greatly overestimated and no revised ^{17}O abundances are available (*21*). Two-zone mixtures of the He/C zone with the He/N, O/Ne, or O/C zones or the H envelope can match the measured $^{18}O/^{16}O$ ratio in S-C122. However, contributions from the O/Ne and O/C zones must be minor because these zones have very high $^{42,44}Ca/^{40}Ca$ and $^{46,47,49,50}Ti/^{48}Ti$ ratios [for example, up to $100 \times (^{50}Ti/^{48}Ti)_{solar}$ for $^{50}Ti/^{48}Ti$ in a 25 $M_\odot$ SN] in contrast to the measured Ti and Ca ratios that are essentially normal. The He/N zone cannot be a major component because this zone has a very low $^{25}Mg/^{24}Mg$ ratio and a high $^{26}Al/^{27}Al$ ratio (*22*), whereas S-C122 has a normal $^{25}Mg/^{24}Mg$ ratio and only an ~10% excess of ^{26}Mg (which could have originally been either ^{26}Mg or ^{26}Al). Contributions from the innermost zones were also minor because there was no measurable excess in ^{44}Ca, the signature of very short-lived ^{44}Ti ($^{44}Ti/^{48}Ti \leq 0.02$), which is a product of explosive nucleosynthesis. Thus, the isotopic signatures of S-C122 indicate that this grain formed primarily from a mixture of materials from the He/C zone and the H envelope. Such a mixture does not work for a 25 $M_\odot$ SNII because the $^{26}Mg/^{24}Mg$ and $^{26}Al/^{27}Al$ ratios are too high in both the He/C zone and the H envelope (*22*); therefore, a 25 $M_\odot$ SNII source seems to be excluded.

The best match was found for a mixture of an ~0.3% He/C zone and a 99.7% H envelope of 15 $M_\odot$SNII, which also gives C/O = 0.4. The exact proportions will depend on improved calculations of the O isotope yields (*17*). Calculated and measured ratios were consistent except for low calculated $^{25}Mg/^{24}Mg$ and $^{50}Ti/^{48}Ti$ ratios (Fig. 2). Whereas the match for ^{50}Ti can be improved by adding a small contribution (~0.2%) of O/C or O/Ne zone material to the mixture, the resulting composition would differ from the measured Mg isotopes.

Oxide grains from AGB stars. The other grains reported here have O isotopic compositions that fall in the range of previously identified presolar oxide grains and are consistent with origins in AGB stars (Fig. 3). Most grains reported here have isotopic compositions that are compatible with the results of the first and the second dredge-up in red

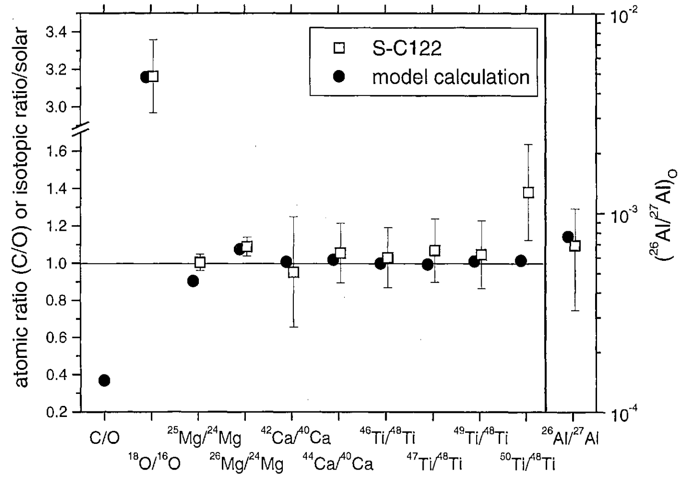

Fig. 2. Isotopic compositions of S-C122 are compared with a mixture of 0.3% He/C zone material with 99.7% H envelope material for a 15 $M_\odot$ SNII [data from (*17*)]. The mixing ratio was chosen to match the $^{18}O/^{16}O$ ratio as described in text. The measured data are reasonably well explained by this mixture except at the $^{25}Mg/^{24}Mg$ and $^{50}Ti/^{48}Ti$ ratios. We have calculated the $^{26}Mg/^{24}Mg$ and $^{26}Al/^{27}Al$ ratios for the mixing model. The $(^{26}Al/^{27}Al)_o$ ratio for S-C122 was inferred by assuming solar Mg isotopes. Error bars in Figs. 2 through 4 indicate ±2σ.

Table 2. Ca and Ti isotopic ratios in presolar corundum grains. The values of the terrestrial samples are from (*39*) for Ca and from (*40*) for Ti; measurements of the sun (solar wind or photosphere) are from (*41*). B39 and Org B data are from (*31*). Dashes indicate not applicable.

Sample	$^{42}Ca/^{40}Ca \pm 2\sigma$	$^{44}Ca/^{40}Ca \pm 2\sigma$	$^{46}Ti/^{48}Ti \pm 2\sigma$	$^{47}Ti/^{48}Ti \pm 2\sigma$	$^{49}Ti/^{48}Ti \pm 2\sigma$	$^{50}Ti/^{48}Ti \pm 2\sigma$
Terrestrial	0.006621	0.021208	0.108548	0.099315	0.074463	0.072418
Sun	0.0057 to 0.0123	0.017 to 0.024	—	—	—	—
S-C122	0.00636 ± 0.00198	0.02271 ± 0.00346	0.1120 ± 0.0175	0.1062 ± 0.0169	0.0780 ± 0.0136	0.1000 ± 0.0185
S-C201	—	—	0.1211 ± 0.0305	0.1194 ± 0.0302	0.0892 ± 0.0247	0.1402 ± 0.0518
S-C203	—	—	0.1040 ± 0.0130	0.0887 ± 0.0118	0.0804 ± 0.0108	0.0897 ± 0.0138
S-C235	—	—	0.1199 ± 0.0305	0.1181 ± 0.0302	0.0882 ± 0.0247	0.1579 ± 0.0518
S-C261	—	—	0.0855 ± 0.0073	0.0811 ± 0.0070	0.0554 ± 0.0054	0.0464 ± 0.0080
B39	—	—	0.1058 ± 0.0050	0.1045 ± 0.0049	0.0754 ± 0.0042	0.0774 ± 0.0116
Org B	—	—	0.1297 ± 0.0020	0.1087 ± 0.0017	0.0805 ± 0.0019	0.0784 ± 0.0022

giant or AGB stars with initial $^{18}O/^{16}O \geq (^{18}O/^{16}O)_{solar}$, whereas most presolar oxide grains that were reported previously appear to have originated from stars with initial $^{18}O/^{16}O \leq (^{18}O/^{16}O)_{solar}$ and often required cool bottom processing (CBP) (Fig. 3). This difference is probably due to differences in search techniques between studies and not to an intrinsic difference in the population of presolar oxide grains between meteorites [see also (*7*)]. If our data represent an unbiased sampling of presolar oxides, then the large fraction of grains with high $^{18}O/^{16}O$ ratios implies that most parent stars had metallicity greater than or equal to solar metallicities (Fig. 3), a situation similar to that for presolar SiC grains (*13*). Two grains (S-C201 and S-C261) have low $^{18}O/^{16}O$ ratios and could be interpreted as the result of the first dredge-up in stars of metallicity ~0.5 $Z_{\odot}$. Alternatively, CBP in higher metallicity stars can produce the same compositions (*23*).

Grain B-C8 is anomalous in its $^{18}O/^{16}O$ ratio but falls near the galactic evolution trend (GET) (Fig. 3B). If the parent star of this grain had an initial O composition on the GET, then it would have been a star with a very low mass ($\leq 1\ M_{\odot}$) and $Z \approx 0.025$. Such a low-mass star has a lifetime of $\geq 10 \times 10^9$ years. It is unlikely that such a high-metallicity star could have formed at such an early stage of the galaxy to provide grains to the solar nebula. For the galaxy as a whole, galactic evolution models predict a monotonic increase in $^{17,18}O/^{16}O$ ratios with time (*24*). However, metallicity and chemical compositions of stars of the same age at the solar galactocentric distance vary by a factor of ~2 (*25*). Similar variations may be expected in isotopic compositions. In addition, the solar $^{18}O/^{17}O$ ratio of 5.2 is higher than the value of 3.5 in the present-day interstellar medium (*26*). Thus, one should expect a band of initial compositions along the GET line. If the initial composition of the parent star of B-C8 was enriched in ^{18}O and depleted in ^{17}O relative to $(^{18}O/^{17}O)_{solar}$ (such as on the line with $^{18}O/^{17}O \approx 10$ in Fig. 3B), it could have been a higher mass star with a much shorter lifetime. Similarly, if B-C72, B-C145, and S-C245 are presolar grains, they probably also originated from stars with high $^{18}O/^{17}O$ ratios.

The $^{25}Mg/^{24}Mg$ ratios in most grains (except for B-C68 and S-S21) are normal within errors (Table 1). Normal $^{25}Mg/^{24}Mg$ ratios of AGB grains with a wide range of metallicities imply that the $^{25}Mg/^{24}Mg$ ratio has not changed for most of galactic history, in contrast with theoretical expectations. Eleven grains have ^{26}Mg excesses [$^{26}Mg/^{24}Mg$ ratios up to $2.3 \times (^{26}Mg/^{24}Mg)_{solar}$]. These large excesses and normal $^{25}Mg/^{24}Mg$ ratios imply an in situ decay of ^{26}Al (mean lifetime $\bar{\tau}$ = 1.05 million years). In AGB stars, ^{26}Al is produced by $^{25}Mg(p, \gamma)^{26}Al$ in the H shell (*27, 28*) and is brought into the envelope during the AGB phase. Three grains with anomalous oxygen (B-C8, B-C155, and S-C13) show little evidence of ^{26}Al and may have formed before the parent stars reached the more advanced AGB stage. The highest $(^{26}Al/^{27}Al)_o$ value found in the present study is 1.7×10^{-3} for S-C201, whose O isotopic composition falls within the region that is accessible by CBP. It has been known that grains with low $^{18}O/^{16}O$ ratios, which are indicative of CBP, also generally have higher $(^{26}Al/^{27}Al)_o$ ratios (*29*). Because the effects of CBP on the $^{18}O/^{16}O$ ratio in the envelope increase as the AGB progresses (*23*) and because the $^{26}Al/^{27}Al$ ratio increases with the number of thermal pulses, the negative correlation between $^{18}O/^{16}O$ and $(^{26}Al/^{27}Al)_o$ ratios implies that grains with lower $^{18}O/^{16}O$ and higher $(^{26}Al/^{27}Al)_o$ ratios formed later than other oxide grains in the evolution of their parent stars.

Three grains (B-C72, B-C145, and S-C245) with excesses in ^{26}Mg have O isotopic compositions that are indistinguishable from solar O. Their $(^{26}Al/^{27}Al)_o$ ratios of 1.5×10^{-4} to 3×10^{-4} are much higher than those of the canonical solar nebula (*30*). There are two possible explanations for these grains. One is that the grains are presolar but have solar O isotopic composition. A solar O composition could be produced by the first dredge-up in stars with initial $^{18}O/^{17}O > (^{18}O/^{17}O)_{solar}$. Another possibility is that these grains could be very early solar nebular condensates. If ^{26}Al were homogeneously distributed in the nebula, these grains would have formed 1 million to 4 million years before Ca-Al–rich inclusions, which have $(^{26}Al/^{27}Al)_o$ ratios up to 5×10^{-5} (*30*).

Titanium compositions were measured for four AGB corundum grains, and these data are shown along with data from grains B39 and Org B (*31*) in Table 2 and Fig. 4. Two grains (S-C201 and S-C235) have large resolvable ^{50}Ti excesses (but with large errors) that are much larger than those found in

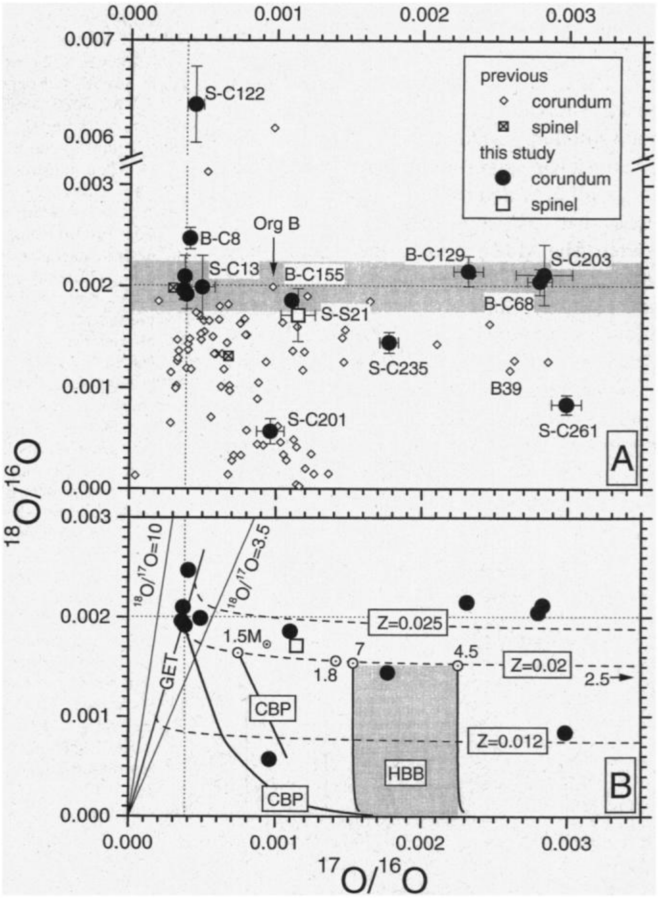

Fig. 3. (**A**) Oxygen isotopic compositions for the presolar oxide grains that were found in this study with preselection by only SEM mapping (larger symbols with error bars) and for the presolar oxide grains that were found in previous studies (*4, 5, 7, 8*). The grains from previous studies were mostly found by an ion-imaging technique (small symbols). Grains from this study are labeled except for those with near-solar O compositions (B-C72, B-C145, and S-C245). Two grains (B39 and Org B) that were previously identified without ion imaging are also labeled. Most of our grains are in the envelope (shaded area), where the ion-imaging technique would not detect them. Dotted lines, solar values. (**B**) Nucleosynthesis in AGB stars. The O isotopic ratios in the envelopes of 1 to 7 $M_{\odot}$ stars after the first dredge-up, which occurs at the end of the main sequence stage of stellar evolution, are shown by dashed lines. Each dashed line represents an array of envelope compositions for stars of different mass and a single metallicity (*Z*) (*42*). Initial compositions were assumed to fall on the GET passing through the solar composition (*24*). The second dredge-up, which occurs at the end of core He burning, has only minor effects on oxygen; the third dredge-up, which is produced by He shell flashes, has a negligible effect (*42*). In stars of 4.5 to 7 $M_{\odot}$, HBB occurs at the base of the convective envelope, destroying most of the ^{18}O (*43*). In stars of 1 to 2.3 $M_{\odot}$, extra mixing below the convective envelope (shaded area) during the red giant and AGB phases (CBP) also lowers the $^{18}O/^{16}O$ ratio, making the areas to the left and right of the HBB region accessible (*23*). Dotted lines, solar values.

presolar SiC (*12*), whereas the other grains show smaller effects, which are compatible with the SiC data. Titanium isotopes in AGB stars are modified by an s-process in the He shell so that ^{46}Ti and ^{49}Ti abundances are increased slightly (^{50}Ti shows a greater increase, ^{48}Ti is decreased, and the ^{47}Ti production factor is almost unity). The Ti yields, particularly for ^{50}Ti, depend critically on the contribution of neutrons from the ^{22}Ne source. The s-process products are mixed into the stellar envelope by the third dredge-up, and the s-process enrichments in the envelope increase (along with the C/O ratio) with the number of thermal pulses. In general, large excesses of ^{50}Ti are not expected. A recent study showed that substantial ^{50}Ti increases were found for advanced AGB stages of intermediate- to high-mass stars (line 5B in Fig. 4) or of low-mass low-metallicity stars (line 1.5B) when $C/O > 1$ (*32*). In stars of >4.5 $M_\odot$, hot bottom burning (HBB) during the third dredge-up reduces the C/O ratio in the envelope and prevents the formation of carbon stars (*33*), which favors oxide production. This may explain why SiC grains from AGB sources do not show similarly large ^{50}Ti effects. It is plausible to attribute the Ti composition of S-C235 to a ~ 5 $M_\odot$ star with HBB; however, the ^{18}O/^{16}O ratio does not appear to support major HBB effects. For S-C201, the Ti and O compositions and the $(^{26}\text{Al}/^{27}\text{Al})_0$ ratio can be explained by a late-stage low-metallicity star ($Z \approx 0.01$), but such a star would have had $C/O > 1$.

Smaller contributions of s-process Ti would be required if the initial compositions of the parent stars were enriched in ^{50}Ti. It has been suggested that ^{46,47,49,50}Ti/ ^{48}Ti ratios increase with increasing metallicity in the galaxy (*24*). Corundum Org B has ^{46,47,49,50}Ti/^{48}Ti ratios that are higher than $(^{46,47,49,50}\text{Ti}/^{48}\text{Ti})_{\text{solar}}$ ratios, and the ^{46,47}Ti enrichments are larger than ^{49,50}Ti, whereas the s-process model predicts larger ^{50}Ti enrichments. The compositions of Ti and O in Org B have been interpreted to indicate a parent star with a metallicity that is higher than solar metallicity (*31*). S-C261 is depleted in all minor Ti isotopes in relation to ^{48}Ti. Such a Ti isotope pattern cannot be produced by AGB stars with solar initial composition, which suggests that the initial ^{46,47,49,50}Ti/ ^{48}Ti ratios of the parent star were lower than $(^{46,47,49,50}\text{Ti}/^{48}\text{Ti})_{\text{solar}}$ ratios. Oxygen isotopes also indicate that S-C261 may come from a low-metallicity star ($Z \approx 0.012$) (Fig. 3B). However, in the other grains, there is no simple correlation in the Ti isotopic patterns and the metallicities that are estimated from O isotopes, which implies that the evolution of Ti isotopes in the galaxy is not monotonic. Isotopic compositions and metallicity could be decoupled by the addition of essentially unprocessed H gas from the galactic halo to average galactic material (*25*).

Presolar spinel and condensation processes in stellar ejecta. Spinel grain S-S21 has $^{17}\text{O}/^{16}\text{O} = 3 \times (^{17}\text{O}/^{16}\text{O})_{\text{solar}}$ and $^{18}\text{O}/^{16}\text{O} = 0.85 \times (^{18}\text{O}/^{16}\text{O})_{\text{solar}}$ and is clearly a circumstellar condensate associated with an AGB source (Fig. 3). It has an Al/Mg ratio of 3.2 ± 0.2. This implies that this grain might be a 2:1 mixture of $MgAl_2O_4$ and Al_2O_3 or a solid solution. Including S-S21, a total of four circumstellar spinel grains have been found (*5–7*), all of which have O isotopic compositions that are compatible with an AGB source. The Al/Mg ratios of these grains vary from 2 to 8. Thus, most of them are not stoichiometric spinels. Spinels are known to allow a substantial solid solution of Al_2O_3 at very high temperature (>1500 K) (*34*). Many presolar corundum grains have relatively high Mg contents. Ten of 14 grains in this study have an Al/Mg ratio between 15 and 75. In contrast, the solubility of MgO in Al_2O_3 is very small (*34*). In a stellar atmosphere with $C/O < 1$, Al_2O_3 would be the first oxide phase to condense. $MgAl_2O_4$ would start to form at ~ 250 K below the condensation temperature of Al_2O_3 by a back-reaction of precondensed Al_2O_3 grains with Mg atoms in the gas (*35*). If this reaction went to completion, all Al_2O_3 would be consumed to form $MgAl_2O_4$. If not, the corundum grains would be only partially reacted to form an aluminous spinel. We conclude that the presolar spinels with nonstoichiometric compositions and presolar corundum grains with high Mg contents represent various stages of back-reaction between the earlier condensed Al_2O_3 crystals and the Mg atoms in the gas phase in an expanding stellar outflow.

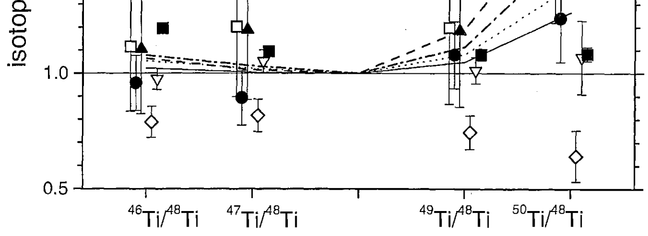

Fig. 4. Ti isotopic ratios of corundum grains associated with AGB sources [four from this study and two from previous studies (*31*)]. Excesses in ^{50}Ti are seen in four grains. In contrast, S-C261 is depleted in all minor Ti isotopes in relation to ^{48}Ti. Model Ti isotopic compositions in the envelope of thermally pulsing AGB stars from solar initial Ti compositions are shown as the following lines, which are designated in the legend: 1.5A (1.5 $M_\odot$, $Z = 0.01$, $C/O = 1$), 1.5B (1.5 $M_\odot$, $Z = 0.01$, $C/O = 2.1$), 5A (5 $M_\odot$, $Z = 0.02$, $C/O = 1$), and 5B (5 $M_\odot$, $Z = 0.02$, $C/O = 1.3$).

References and Notes

1. E. Zinner, in *Astrophysical Implications of the Laboratory Study of Presolar Materials*, T. J. Bernatowicz and E. Zinner, Eds. (American Institute of Physics, Woodbury, NY, 1997), pp. 3–26.
2. U. Ott, *Nature* **364**, 25 (1993).
3. G. R. Huss, I. D. Hutcheon, G. J. Wasserburg, J. Stone, *Lunar Planet. Sci.* **XXIII**, 563 (1992).
4. I. D. Hutcheon, G. R. Huss, A. J. Fahey, G. J. Wasserburg, *Astrophys. J.* **425**, L97 (1994); G. R. Huss, A. J. Fahey, R. Gallino, G. J. Wasserburg, *ibid.* **430**, L81 (1994).
5. L. R. Nittler, C. M. O. D. Alexander, X. Gao, R. M. Walker, E. K. Zinner, *Nature* **370**, 443 (1994).
6. R. Strebel, P. Hoppe, P. Eberhardt, *Meteorit. Planet. Sci.* **31**, A136 (1996).
7. L. R. Nittler *et al.*, *Astrophys. J.* **483**, 475 (1997).
8. L. R. Nittler and R. Cowsik, *Phys. Rev. Lett.* **78**, 175 (1997); L. R. Nittler, C. M. O'D. Alexander, J. Wang, X. Gao, *Nature* **393**, 222 (1998).
9. We use the terms "solar" or "normal" to refer to bulk solar system isotopic compositions of the elements. Because direct measurements of the solar composition have such large errors and because terrestrial values agree within errors (Tables 1 and 2), we use the terrestrial values for comparisons in this paper.
10. M. Heinrich, G. R. Huss, G. J. Wasserburg, *Lunar Planet. Sci.* **XXIX**, 1715 (1998).
11. Bishunpur (LL3.1) and Semarkona (LL3.0) are unequilibrated ordinary chondrites.
12. P. Hoppe, S. Amari, E. Zinner, T. Ireland, R. S. Lewis, *Astrophys. J.* **430**, 870 (1994).
13. G. R. Huss, I. D. Hutcheon, G. J. Wasserburg, *Geochim. Cosmochim. Acta* **61**, 5117 (1997).
14. Analytical procedures for O and Mg are similar to those in (*4*). Titanium and Ca isotopes were measured with an O^- primary beam and a mass-resolving power of 1300. Major interferences were monitored and corrected. For example, ^{52}Cr was monitored to correct the ^{50}Cr interference on ^{50}Ti. The ^{50}Cr/^{52}Cr ratio was assumed to be solar within 10%. All measurement uncertainties were propagated into the final results. All errors reported are $\pm 2\sigma$.
15. M. Arnould, G. Meynet, G. Paulus, in *Astrophysical Implications of the Laboratory Study of Presolar Materials*, T. J. Bernatowicz and E. Zinner, Eds. (American Institute of Physics, Woodbury, NY, 1997), pp. 179–202.
16. Although Al_2O_3 is thermodynamically stable at $C/O > 1$, the formation temperatures are 500 to 1000 K lower than those at $C/O < 1$, and the stability ranges are very narrow (*35*). Thus, $C/O < 1$ is the favorable condition for the formation of corundum.
17. S. E. Woosley and T. A. Weaver, *Astrophys J. Suppl. Ser.* **101**, 181 (1995).
18. G. J. Wasserburg, R. Gallino, M. Busso, *Astrophys. J.* **500**, L189 (1998).
19. C. Travaglio *et al.*, *ibid.*, in press.
20. B. S. Meyer, T. A. Weaver, S. E. Woosley, *Meteoritics* **30**, 325 (1995).
21. S. E. Woosley, R. D. Hoffman, F. X. Timmes, T. A. Weaver, F.-K. Thielemann, in *Nuclei in the Cosmos IV*,

J. Görres, Ed. (Elsevier, Amsterdam, 1997), pp. 445–452. The ^{18}O yields in (*17*) will also be subject to substantial revisions, but the location where ^{18}O is produced (the He/C zone) will not change and should provide a basis for making a semiquantitative assessment of the material contribution from the various zones.

22. Magnesium and Al isotopes in the He/C and He/N zones and in the H envelope mainly reflect proton reactions occurring in the H-burning shell. In the He/N zone, the $^{25}Mg/^{24}Mg$ ratio is less than 10% of its initial value, and the $^{26}Al/^{27}Al$ ratio is as high as 0.5 because of $^{25}Mg(p, \gamma)^{26}Al$ (*17*). Thus, a mixture of materials from the He/C and He/N zones would have a much smaller $^{25}Mg/^{24}Mg$ ratio and a much higher $^{26}Al/^{27}Al$ ratio than those of S-C122. In a 25 $M_{\odot}$ SNII, the $^{26}Mg/^{24}Mg$ ratio is $\sim 2 \times (^{26}Mg/^{24}Mg)_{solar}$ in the He/C zone and $\sim 1.15 \times (^{26}Mg/^{24}Mg)_{solar}$ in the H envelope. The $^{26}Al/^{27}Al$ ratios are $\sim 4 \times 10^{-3}$ and $\sim 2 \times 10^{-2}$ in the He/C zone and the H envelope, respectively. Thus, grains from a mixture of materials from the H/C zone and the H envelope in a 25 $M_{\odot}$ SNII would have a much higher excess of ^{26}Mg than S-C122.
23. G. J. Wasserburg, A. I. Boothroyd, I.-J. Sackmann, *Astrophys. J.* **447**, L37 (1995).
24. F. X. Timmes, S. E. Woosley, T. A. Weaver, *Astrophys J. Suppl. Ser.* **98**, 617 (1995).
25. B. Edvardsson *et al.*, *Astron. Astrophys.* **275**, 101 (1993).
26. P. G. Wannier, in *The Center of the Galaxy*, M. Morris, Ed. (Kluwer Academic, Dordrecht, Netherlands, 1989), pp. 107–119.
27. M. Forestini, G. Paulus, M. Arnould, *Astron. Astrophys.* **252**, 597 (1991).
28. R. Gallino, C. M. Raiteri, M. Busso, F. Matteucci, *Astrophys. J.* **430**, 858 (1994).
29. L. R. Nittler, in *Astrophysical Implications of the Laboratory Study of Presolar Materials*, T. J. Bernatowicz and E. Zinner, Eds. (American Institute of Physics, Woodbury, NY, 1997), pp. 59–82.
30. T. Lee, D. A. Papanastassiou, G. J. Wasserburg, *Geophys. Res. Lett.* **3**, 109 (1976); *Astrophys. J.* **211**, L107 (1977).
31. G. R. Huss, A. J. Fahey, G. J. Wasserburg, *Meteoritics* **29**, 475 (1994).
32. M. Lugaro, R. Gallino, M. Busso, S. Amari, E. Zinner, in preparation.
33. A. I. Boothroyd, I.-J. Sackmann, S. C. Ahern, *Astrophys. J.* **416**, 762 (1993).
34. B. Hallstedt, *J. Am. Ceram. Soc.* **75**, 1497 (1992).
35. J. M. Lattimer, D. N. Schramm, L. Grossman, *Astrophys. J.* **219**, 230 (1978).
36. C. Holmden, D. A. Papanastassiou, G. J. Wasserburg, *Geochim. Cosmochim. Acta* **61**, 2253 (1997); R. Baertschi, *Earth Planet. Sci. Lett.* **31**, 341 (1976).
37. E. J. Catanzaro, T. J. Murphy, E. L. Garner, W. R. Shields, *J. Res. Natl. Bur. Stand.* **70A**, 453 (1966).
38. M. R. Collier *et al.*, *J. Geophys. Res.* **103**, 7 (1998); R. S. Selesnick *et al.*, *Astrophys. J.* **418**, L45 (1993) and references therein.
39. F. R. Niederer and D. A. Papanastassiou, *Geochim. Cosmochim. Acta* **48**, 1279 (1984).
40. F. R. Niederer, D. A. Papanastassiou, G. J. Wasserburg, *Geochim. Cosmochim. Acta* **49**, 835 (1985).
41. R. Kallenbach *et al.*, *Astrophys. J.* **498**, L75 (1998).
42. A. I. Boothroyd, I.-J. Sackmann, G. J. Wasserburg, *Astrophys. J.* **430**, L77 (1994); J. C. Lattanzio and A. L. Boothroyd, in *Astrophysical Implications of the Laboratory Study of Presolar Materials*, T. J. Bernatowicz and E. Zinner, Eds. (American Institute of Physics, Woodbury, NY, 1997), pp. 85–114.
43. A. I. Boothroyd, I.-J. Sackmann, G. J. Wasserburg, *Astrophys. J.* **442**, L21 (1995).

44. We thank S. E. Woosley and T. A. Weaver for generously providing us with their SNII data in a computer-readable format and the reviewers for their valuable comments and suggestions. The study was supported by NASA grant NAG 5-4083. This is California Institute of Technology's Division of Geological and Planetary Sciences contribution 8523(1004).

26 June 1998; accepted 8 October 1998